Russian Geology and Geophysics © 2020, V.S. Sobolev IGM, Siberian Branch of the RAS
Vol. 61, No. 5–6, pp. 663–674, 2020 *DOI:10.15372/RGG2020103* *Geologiya i Geofizika*

Composition of Reduced Mantle Fluids: Evidence from Modeling Experiments and Fluid Inclusions in Natural Diamond

A.G. Sokol[a,b,] ✉, A.A. Tomilenko[a], T.A. Bul'bak[a], I.A. Sokol[a], P.A. Zaikin[c], N.V. Sobolev[a,b]

[a] *V.S. Sobolev Institute of Geology and Mineralogy, Siberian Branch of the Russian Academy of Sciences, pr. Akademika Koptyuga 3, Novosibirsk, 630090, Russia*

[b] *Novosibirsk State University, ul. Pirogova 1, Novosibirsk, 630090, Russia*

[c] *N.N. Vorozhtsov Institute of Organic Chemistry, Siberian Branch of the Russian Academy of Sciences, pr. Akademika Lavrentieva 9, Novosibirsk, 630090, Russia*

Received 31 January 2020; accepted 23 March 2020

Abstract—Experimental modeling in the C–O–H, C–O–H–N, and peridotite–C–O–H–N systems, combined with analyses of fluid inclusions in natural diamonds, is used to reconstruct the compositions of fluids that can be stable in the reduced mantle. Hydrocarbons (HCs) in the upper mantle can form either by reactions of carbonates with iron/wüstite and water or by direct hydrogenation of carbon phases (graphite, diamond, and amorphous carbon) interacting with reduced fluids. Carbon required for the formation of HCs can come from diamond, graphite, or carbonates. Mainly light alkanes are stable at the mantle pressures and temperatures in the C–O–H and C–O–H–N systems as well as in the peridotite–fluid system under ultrareduced to moderately reduced redox conditions at the oxygen fugacity from –2 to +2.5 lg units relative to the IW (Fe–FeO) buffer. Some oxygenated HCs can be stable in fluids equilibrated with carbonate-bearing peridotite. Ammonia and, to a lesser degree, methanimine (CH_3N) are predominant nitrogen species in reduced fluids in the conditions of the subcratonic lithosphere or the Fe^0-bearing mantle.

The presence of HCs as common constituents of reduced mantle fluids is supported by data on inclusions from natural diamonds hosted by kimberlites of the Yakutian province and from placer diamonds of the northeastern Siberian craton and the Urals. Fluid inclusions have minor amounts of H_2O, methane, and other light alkanes but relatively high concentrations of oxygenated hydrocarbons, while the H/(H + O) ratio varies from 0.74 to 0.93. Hydrocarbon-bearing fluids in some eclogitic diamonds have high CO_2 concentrations. Also, the fluid inclusions have significant percentages of N_2 and N-containing species, Cl-containing HCs, and S-containing compounds.

Both the experimental results and the analyses of fluid inclusions in natural diamonds indicate that HCs are stable in the upper mantle conditions. The set of hydrocarbons, mainly light alkanes, might have formed in the mantle from inorganic substances. Further research should focus on the causes of the difference between experimental and natural fluids in the contents of methane, light alkanes, oxygenated hydrocarbons, and water and on the stability of N-, S-, and Cl-containing fluid components.

Keywords: mantle, fluid, inclusions in diamond, hydrocarbons, deep cycle of carbon and nitrogen

INTRODUCTION

The fluid phase stable in the Earth's mantle is a key link in the deep cycle of volatiles, and knowledge of its composition is indispensable for reconstructions of the crust and mantle history and deep-seated mineral formation (Sobolev, 1960; Kadik, 2003; Etiope and Sherwood Lollar, 2013; Shirey et al., 2013; Luth, 2014). In this respect, the results of experiments at high pressures and temperatures and low oxygen fugacity (f_{O_2}), along with evidence on fluid inclusions in natural diamonds, have important implications for the composition of fluids that are stable under the mantle conditions. Progress in understanding the deep cycles of carbon, hydrogen, and nitrogen became possible lately as better constraints have been obtained for the physicochemical properties of H_2O, CO_2, CH_4, and NH_3 at high pressures and temperatures. Meanwhile, many problems concerning the formation mechanisms and stability of HC and nitrogen species in deep fluids, in a large range of P–T–f_{O_2}–f_{H_2} values, remain unresolved.

Studies in the course of two recent decades (Frost et al., 2004; Rohrbach et al., 2007; Frost and McCammon, 2008; Rohrbach and Schmidt, 2011) have shown that mantle below 250 km has low f_{O_2} corresponding to the stability of metal in peridotite (Fig. 1). The transport of this reduced mantle material to shallower depths by the global mantle convection may bring about changes in the composition of fluid and other phases that accumulate volatiles. As evidenced by data on mantle xenoliths (Woodland and Koch, 2003; Goncharov et al., 2012; Yaxley et al., 2012; Stagno et

✉ Corresponding author.
E-mail address: sokola@igm.nsc.ru (A.G. Sokol)

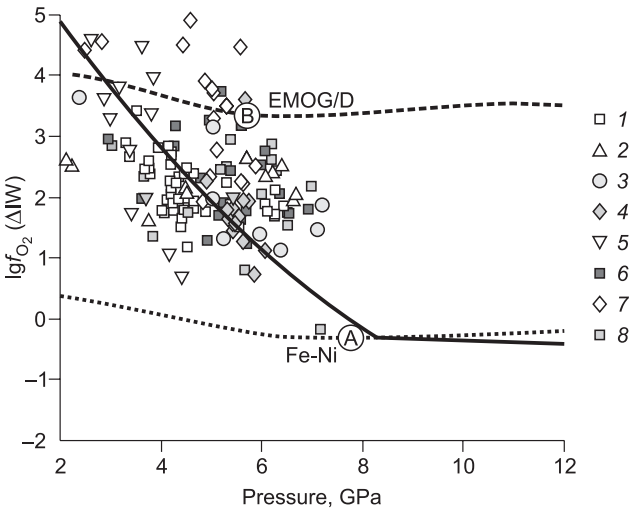

Fig. 1. Calculated oxygen fugacity for mantle xenoliths (Stagno et al., 2013) from kimberlites of different cratons: *1–5*, Kaapvaal (Luth et al., 1990; Canil and O'Neill, 1996; Woodland and Koch, 2003; Creighton et al., 2009; Lazarov et al., 2009); *6*, *7*, Slave (McCammon and Kopylova, 2004; Creighton et al., 2010); *8*, Siberia (Yaxley et al., 2012). f_{O_2} are plotted in lg coordinates relative to the IW buffer (lgf_{O_2}[ΔIW]). The curves of metal deposition in peridotite (blue, Fe-Ni), enstatite–magnesite–olivine–graphite/diamond buffer (green, EMOG/D), and f_{O_2} decrease with pressure in subcratonic peridotite mantle (red) are after (Frost and McCammon, 2008). A and B in circles mark the conditions of experiments with the lherzolite–C–O–H–N system (Sokol et al., 2018b).

al., 2013), f_{O_2} in mantle rocks ascending to 120–150 km may reach the enstatite–magnesite–olivine–graphite/diamond equilibrium (EMOG/D buffer), which leads to oxidation of volatiles and generation of carbonate melts (Stagno et al., 2013). Thus, the fluid regime under adiabatic decompression during mantle upwelling from ~250 km to 120–150 km (Fig. 1) is controlled by successive changes of the petrological systems: (1) Fe^0-bearing peridotite–reduced fluid; (2) peridotite–fluid; (3) carbonated peridotite–oxidized fluid/melt.

The redox stability of N-bearing components in the C-O-H-N system has implications for nitrogen transport to mantle depths (Busigny et al., 2003; Elkins et al., 2006; Halama et al., 2010; Bebout et al., 2016; Zerkle and Mikhail, 2017; Mallik et al., 2018; Mysen, 2019). The presence of NH_3 in the fluid can provide the $K^+ \rightarrow (NH_4^+)$ substitution in micas and other potassic minerals at high pressures and temperatures and thus maintain nitrogen transport with slabs in subduction zones (Watenphul et al., 2009, 2010; Li and Keppler, 2014; Luth, 2014; Mikhail and Sverjensky, 2014). Ammonia is known to be stable in the fluid at the mantle pressures and temperatures only at f_{O_2} near the IW buffer (Li and Keppler, 2014; Luth, 2014; Mysen, 2019), but the specific P–T–f_{O_2}–f_{H_2} conditions of NH_3 stability, especially at >4 GPa, remain poorly investigated.

We review the results of recent experiments at the mantle P–T parameters in order to reconstruct (i) the compositions of reduced fluids containing HCs and NH_3 in both simple model systems and in complex natural rock-fluid systems and (ii) oxidation trends of HCs and NH_3 in lithospheric mantle. The experimental evidence is compared with new data on fluid inclusions in natural kimberlitic diamond from the Yakutian province and in placer diamonds from the northeastern Siberian craton and the Ural Mountains.

EXPERIMENTAL APPROACHES

Much progress has been achieved lately in constraining experimentally the composition of reduced fluids and mechanisms of their generation under mantle P–T conditions (Table 1). Numerous experiments were carried out at pressures from 1 to 80 GPa and temperatures from 300 to >2000 °C, with special focus on the upper mantle ranges of 2.5–7.0 GPa and 1000–1400 °C. High pressure was maintained in multianvil, piston cylinder apparatus, or diamond anvil cells (DAC). Samples were placed in capsules made of noble metals (Pt and Au) or iron (steel), and gases (CH_4 and H_2) were introduced into the diamond anvils using a high-pressure gas loading system. Fedorov et al. (1991), in their pioneering experimental study, used TiH_2 as a source of hydrogen for HC synthesis. Hydrogen fugacity (f_{H_2}) in the experiments with high-pressure cells was either unbuffered or buffered at Fe–FeO + H_2O (IW + H_2O) or Mo–MoO_2 + H_2O (MMO + H_2O) equilibria. The conditions of f_{H_2} buffering were discussed in detail in several publications (Matveev et al., 1997; Sokol et al., 2009; Litasov et al., 2014; Sokol et al., 2019a). In the experiments reported by Matveev et al. (1997), f_{H_2} was buffered by WC–WO_2–C + H_2O (WCO + H_2O) and SiC–SiO_2–C + H_2O (SiC + H_2O). The buffers make up the f_{H_2} descending series SiC + H_2O >> IW + H_2O > MMO + H_2O ≈ WCO + H_2O. A highly oxidized buffer of Fe_3O_4 – Fe_2O_3 + H_2O (MH + H_2O) was used in our study of HC fluid oxidation mechanisms (Sokol et al., 2018a). The composition of N-rich reduced fluids was studied using the classical high-pressure cells and f_{H_2} buffers, but has received quite little attention though (Li and Keppler, 2014; Sokol et al., 2017b; 2018a,b).

The starting fluid-generating compounds in the high-pressure experiments either contained organic matter (alkanes or oxygenated HCs) or were originally free from organics (Table 1). The first group included methane, heavy alkanes (docosane), polycyclic aromatic HCs (anthracene), and carboxylic (stearic) acid. Methane exposed to high pressures and temperatures in DAC produced as a rule a methane-rich equilibrium fluid at the account of partial decomposition reactions and condensation. The HC fluid generation occurred by thermal destruction of the starting compounds: heavy alkane, aromatic HC, and carboxylic acid. The HC-free fluid sources comprised substances which maintained inorganic synthesis of hydrocarbons by chemical reactions. The carbon sources included carbonate ($CaCO_3$, $MgCO_3$, $Ca(Fe_{0.5}Mg_{0.5})(CO_3)_2$), or graphite, diamond, or ^{13}C; hydro-

Table 1. Hydrocarbon fluids under mantle *P–T* conditions: experimental approaches and fluid compositions

Reference	HC source	Run conditions				Analysis	Composition of HC-bearing fluid
		HP cell/ capsule	*P*, GPa	*T*, °C, K	f_{H_2} buffer		
(Fedorov et al., 1991)	$C_{14}H_{10} \pm H_2O$	Pt	2.5–4.0	1300–1440 °C	TiH_2	GC	CH_4 90%; C_2H_6 5%; C_3H_8 1–2% (mol.%)
(Matveev et al., 1997)	$C_{18}H_{36}O_2$	Au	2.4	1273 K	SiC IW WCO	GC	CH_4 90%; C_2H_6 2%; H_2O 1.5%; H_2 6% CH_4 80%; C_2H_6 2%; H_2O 12%; H_2 5% CH_4 70%; C_2H_6 1.5%; H_2O 30%; H_2 4% (mol.%)
(Benedetti et al., 1999)	CH_4	DAC	5.5	2000–3000 K	–	FTIR, Raman	$CH_4 \rightarrow C + HCs$ (C_xH_y)
(Kenney et al., 2002)	$CaCO_3 + FeO + H_2O$	Pt, Fe	1–5	≤1500 °C	–	MS	At 5 GPa, C_1–C_6 alkanes, predominant CH_4
(Scott et al., 2004)	$CaCO_3 + FeO + H_2O$	DAC	5.7	1500 °C	–	Raman	CH_4
(Sokol et al., 2004)	$C_{14}H_{10} + H_2O$	Pt, Au	5.5	1200–1420 °C	–	GC	CH_4 17%; H_2O 79%; H_2 0.9%; CO_2 2.4% (mol.%)
(Kolesnikov et al., 2009)	CH_4, C_2H_6	DAC	2–14	1000–2500 K		Raman	CH_4 ® C + H_2 + C_2H_6 + C_3H_8 + C_4H_{10}
(Sharma et al., 2009)	Graphite + H_2 $CaCO_3 + FeO + H_2O$	DAC	5.0–6.5	>1500 °C 620 °C	–	Raman	$CH_4 + H_2$ $CO_2 \sim H_2O > CH_4$
(Sokol et al., 2009)	$C_{18}H_{36}O_2$ $C_{22}H_{46}$	Pt	6.3	1400–1600 °C	MMO	GC	H_2O 60–70%; H_2 25–30%; CH_4 2%; C_2H_6 1% H_2 50%; CH_4 30–45%; C_2H_6 6–9%; C_3H_8 3–4% (mol.%)
(Kucherov et al., 2010)	$CaCO_3 + Fe + H_2O$ Graphite + Fe + H_2O	Pt	5.0	1500 K	–	GC	CH_4 72%; C_2H_6 25%; C_3H_8 2–3% CH_4 93–98%; C_2H_6 0–6%; C_3H_8 > 0.5% (mol.%)
(Lobanov et al., 2013)	CH_4	DAC	1.7–80	300–2000 K		Raman	CH_4 at upper mantle *P–T* parameters, alkanes with H/C ~ 2 at lower mantle *P–T* parameters
(Sonin et al., 2014)	$CaCO_3 + Ca(OH)_2 + Fe$ $MgCO_3 + Ca(OH)_2 + Fe$ $MgCO_3 + Ca(OH)_2 + Fe + SiO_2$	Pt	4.5 4.0 3.0	1600 °C 1400 °C 1400 °C	–	GC–MS	$H_2O > CH_4$ $CO_2 > CH_4 > H_2O$ $H_2O > CH_4 > C_9$–C_{10} aldehydes > C_{12}–C_{16} alkanes
(Mukhina et al., 2017)	$CaCO_3 + FeO + H_2O$	Fe	2.0–6.6	250–600 °C	–	GC Raman	at *T* > 250 °C, alkanes $C_1 > C_2 > C_3 > C_4$ + heavy HCs
(Sokol et al., 2017a)	$C_{22}H_{46}$ $C_{18}H_{36}O_2$	Pt Au	6.3	1100–1400 °C	MMO –	GC–MS	Alkanes C_1 (20–50 rel.%) » C_2 (30–73 rel.%) > C_3 » $H_2O > C_4$ $H_2O > C_1$ » $C_2 > C_3 > C_4$
(Matjuschkin et al., 2019)	Ol + Opx + $C_{18}H_{36}O_2$	Au	3.0–5.0	1150–1280 °C	IW, MMO	Raman	CH_4, H_2, C_2H_6, H_2O?
(Sokol et al., 2018a)	Lherzolite + $C_{22}H_{46}$ Lherzolite + $C_{18}H_{36}O_2$	Pt, Au	5.5–7.8	1150–1350 °C	IW, MMO MH	GC–MS	Alkanes C_1 » $C_2 > H_2O > C_3 > C_4$ » O-containing organics > alkenes $H_2O > CO_2$ (Ol carbonation) > CH_4 » C_2H_6, C_9 carboxylic acids
(Sokol et al., 2018c)	Ol + $C_{22}H_{46}$ Ol + $C_{18}H_{36}O_2$	Au	6.3	1200 °C	MMO	GC–MS	Alkanes $C_1 > C_2 > C_3 > H_2O > C_4$ $H_2O > C_1$,C_9–C_{14} carboxylic acids » $CH_4 > C_2H_6 > C_{14}$–C_{17} alkanes
(Tao et al., 2018)	$Ca(Fe_{0.5}Mg_{0.5})(CO_3)_2 + H_2O$	Au	1.0–6.0	600–1200 °C		GC	CO_2 > alkanes $C_1 > C_2 > C_3 > C_4$, H_2O?
(Sokol et al., 2019a)	^{13}C, diamond, graphite ± CO_2 ± H_2O	Pt, Au	5.5–7.8	1100–1400 °C	IW, MMO	GC–MS	Alkanes C_1 » $C_2 > H_2O$ » $C_3 > C_4$ » O-containing organics > alkenes

GC, gas chromatography; GC–MS, gas chromatography–mass spectrometry; FTIR, Fourier transform infrared spectroscopy; Raman, Raman spectroscopy;
Ol, olivine; Opx, orthopyroxene; DAC, diamond anvil cell. Buffers: WCO, WC–WO_2–C; IW , Fe–FeO; SiC, SiC–SiO_2–C; MMO, Mo–MoO_2 (water was added to all buffers); MH, Fe_3O_4–Fe_2O_3. TiH_2, the source of hydrogen (not a buffer); $C_{14}H_{10}$, anthracene; $C_{18}H_{36}O_2$, stearic acid; $C_{22}H_{46}$, docosane. GC–MS results are given in rel.%.

gen inputs were provided by reactions of wüstite (FeO) or Fe^0 and water or by the hydrogen buffer.

N-rich fluids were generated using an aqueous solution of ammonia (Li and Keppler, 2014; Li et al., 2015), silver azide (AgN_3) (Li et al., 2015), NH_3-bearing minerals, like buddingtonite ($NH_4AlSi_3O_8$)) (Watenphul et al., 2009, 2010; Li et al., 2013), or melamine ($C_3H_6N_6$) (Sokol et al., 2017b; 2018a,b).

The fluid compositions were studied with different approaches. The fluids generated in DAC experiments were analyzed semi-quantitatively by Raman spectroscopy. In the case of classical high-pressure experiments, the fluids obtained in Pt, Au or iron capsules were quenched at >100 deg/s. The re-equilibration of fluid components almost stopped at those quenching rates (Matveev et al., 1997; Sokol et al., 2009, 2017a; Li and Keppler, 2014; Kolesnikov et al., 2017). After the end of the runs, the capsules were placed into a gas chromatograph or a gas chromatograph coupled with a mass spectrometer (Table 1). The former determined quite few elements, whereas the latter resolved up to 300 components, the full scope of synthesized hydrocarbons. In some studies (e.g., Li and Keppler, 2014; Matjuschkin et al., 2019), the fluid composition was determined by Raman spectroscopy of fluid inclusions in minerals (commonly, in olivine).

MAIN SPECIES OF REDUCED FLUIDS

The available experimental and petrolgical data show that hydrocarbons and water are main constituents of reduced fluids (Luth, 2014). The experiments prove the possibility for the generation of hydrocarbons upon interaction of different carbon donors (carbonates, graphite, diamond, and amorphous carbon) with hydrogen generated by the reaction of Fe^0 or FeO with water (Table 1). Important data were obtained by studies of interactions in the systems 'carbonate ($CaCO_3$, $MgCO_3$, $Ca(Fe_{0.5}Mg_{0.5})(CO_3)_2$) – FeO/Fe^0 – H_2O' (Kenney et al., 2002; Scott et al., 2004; Sharma et al., 2009; Kucherov et al., 2010; Sonin et al., 2014; Mukhina et al., 2017), which produce a mixture of light alkanes dominated by CH_4 at the upper mantle *P–T* parameters (Table 1). Such systems with water-rich fluids can produce notable amounts of oxygenated organics like C_9–C_{10} aldehydes and heavy (C_{12}–C_{16}) alkanes (Sonin et al., 2014). Methane and light alkanes can form by reactions of $CaCO_3$ with FeO and H_2O, even under a thermal regime of cold subduction (Mukhina et al., 2017). Synthesis of complex HC systems under the mantle pressures and temperatures requires a carbon donor, a hydrogen donor, and reduced redox conditions, as it was inferred from a review of data on HC generation by reactions with carbonates as a carbon source (Kolesnikov et al., 2017).

Recent experiments at 5.5–7.8 GPa and 1100–1400 °C performed to study the mechanism of HC generation by a reaction between an H-bearing fluid with ^{13}C amorphous carbon, graphite, and diamond (Sokol et al., 2019a) yielded fluids containing light alkanes, minor amounts of alkenes, and oxygenated HCs. Synthesis of isotopically pure ^{13}C alkanes by a reaction of amorphous carbon with an H-bearing fluid proved the possibility of HC formation from inorganic C^0 at the *P–T* parameters corresponding to the upper mantle. In 6.3 GPa runs at 1200–1400 °C, the fluid-graphite reaction rate grew progressively, and the process became avalanche-like as the run duration exceeded 1 h. The amount of fluid generated in a 10-hr run at 1400 °C was two orders of magnitude greater than that at 1 hr run, though twice less at a lower temperature of 1200 °C and the same duration. The HC fluid synthesized at higher pressures and temperatures contained less methane and slightly more alkenes and oxygenated HCs. The yield of HCs from the reaction of hydrogen with diamond was smaller than with any other carbon donors we used. Experiments with CO_2 and $H_2{}^{17}O$ added to the samples have demonstrated that HCs formed by direct hydrogenation of amorphous carbon, graphite, and diamond.

Hydrogen is the major agent in the formation of hydrocarbons, but its concentration is minor in mantle fluids at high *P–T* parameters and low oxygen fugacity. According to gas chromatography, the concentrations of hydrogen (Table 1) are from 4 to 6 mol.% in a C–O–H fluid at 2.4 GPa and 1000 °C, and at f_{H_2} buffered by $SiC + H_2O$, $IW + H_2O$ and $WCO + H_2O$ equilibria (Matveev et al., 1997); may notably exceed 10% in almost H_2O-free ultra-reduced fluids at 6.3 GPa and 1400–1600 °C and at very low f_{O_2} uncommon to the upper mantle (Sokol et al., 2009); but are apparently within a few percent at f_{O_2} about IW, i.e., at the conditions of wet metal-bearing mantle.

The summarized experimental results on synthesis of HCs, thermal destruction of heavy HCs and carboxylic acids, and on the stability of methane (Table 1) show that fluids containing methane, water, light C_2–C_4 alkanes, hydrogen, and oxygenated HCs (listed in decreasing order of contents) can be stable at the pressure, temperature, and oxygen fugacity values corresponding to the upper mantle conditions (Matveev et al., 1997; Benedetti et al., 1999; Sokol et al., 2004, 2009, 2017a, 2018a,c 2019a,b; Kolesnikov et al., 2009, 2017; Kucherov et al., 2010; Lobanov et al., 2013). Note that the relative percentages of main fluid components may vary depending on *P–T–*f_{H_2} conditions (Figs. 1, 2). As shown by the experiments, fluids rich in CH_4 and H_2O, with a notable amount of light alkanes, are stable at f_{H_2} near the IW + H_2O buffer, at the upper mantle pressures and temperatures. Temperature increase at these redox conditions is favorable for partial dissociation of methane with the formation of C^0 (graphite or diamond), hydrogen, and C_2–C_4 alkanes (Kolesnikov et al., 2009; 2017; Sokol et al., 2017a), while the increase in pressure and temperature till the lower mantle values may lead to heavier compositions of alkanes till H/C~2 (Lobanov et al., 2013).

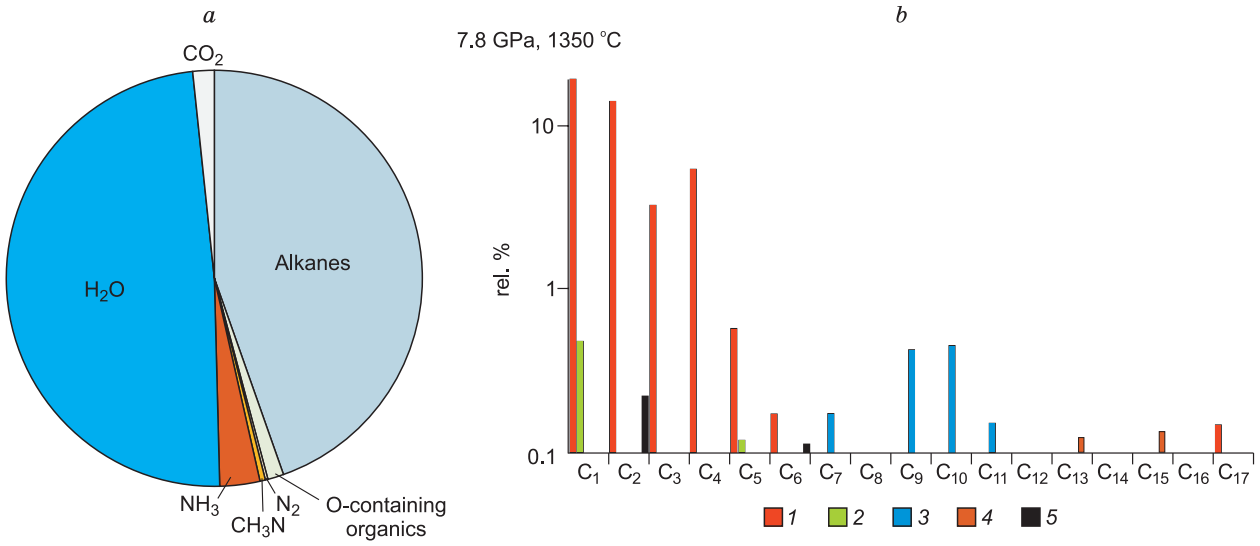

Fig. 2. Composition of quenched fluid from a sample of metal-bearing lherzolite, after (Sokol et al., 2018a). The run conditions are marked by encircled A in Fig. 1. *a*, relative percentages of main C and N components in fluid; *b*, concentrations of alkanes and oxygenated HCs.

Relatively oxidized HC fluids contain more H_2O and CO_2 but less methane. The fluid in experiments with the C–O–H system at 2.4 GPa and 1000 °C (Matveev et al., 1997) changed its composition with increasing f_{O_2} from mainly CH_4–H_2O with minor C_2H_6 to mainly aqueous, and on to H_2O–CO_2. The N-poor C–O–H–N system decreased in methane, to almost zero, while the contents of heavy alkanes changed insignificantly as H_2O increased to >90 rel.% and f_{O_2} reached +2.5 lg f_{O_2} ΔIW (Sokol et al., 2017a). The fluids obtained in experiments with the "lherzolite–C–O–H–N" system (Sokol et al., 2018a), at gradually increasing f_{O_2} and decreasing *P*–*T* parameters, which simulated the ascent of an HC fluid through peridotitic mantle (Figs. 1, 2), were equilibrated successively with three main types of mineral assemblages: Fe^0-bearing lherzolite → lherzolite → magnesite-bearing lherzolite. The fluid equilibrated with metal-bearing lherzolite was found out to consist of methane and ethane and minor amounts of other light alkanes, H_2O, and nitrogen species of ammonia NH_3 and methanimine CH_3N (Fig. 2). Fe^0 became unstable in the system if the fluid contained >40 rel.% H_2O. As f_{O_2} increased to the values of carbon-saturated maximum H_2O content for C–O–H fluids (water maximum, CW), the fluid equilibrated with lherzolite contained notably larger amounts of oxygenated HCs, espe-

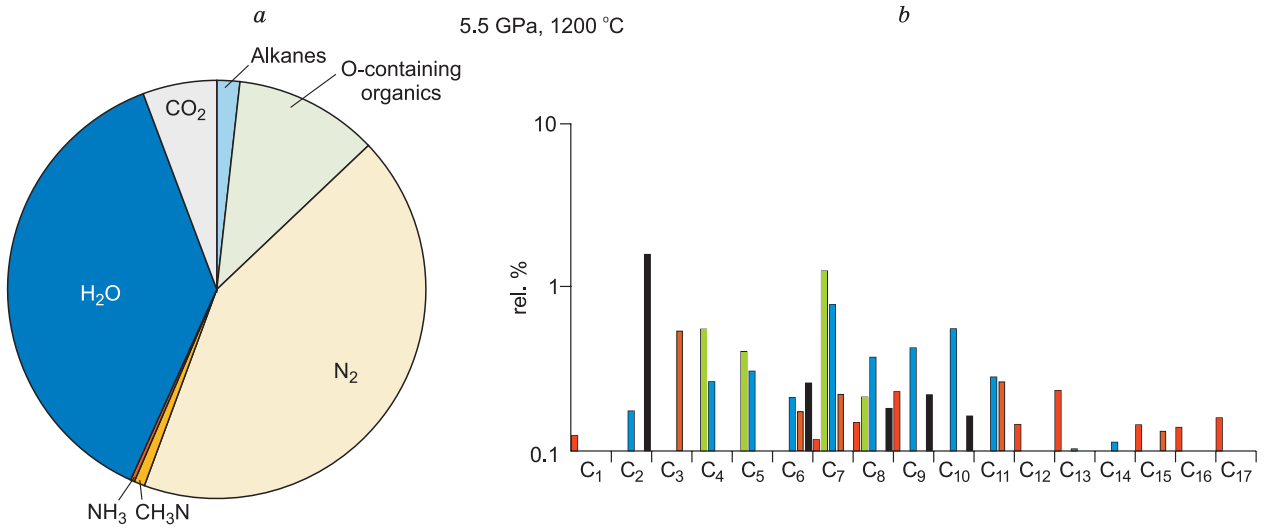

Fig. 3. Composition of quenched fluid from a sample of carbonate-bearing lherzolite, after (Sokol et al., 2018a). The run conditions are marked by encircled B in Fig. 1. *a*, Relative percentages of main C and N components in fluid. High contents of N_2 are due to oxidation of HCs and carbonation of olivine and orthopyroxene; *b*, concentrations of alkanes and oxygenated HCs.

cially methanole and acetic acid, than the fluid in the C–O–H–N system. The fluid equilibrated with carbonate-bearing lherzolite at f_{O_2} about the EMOD (enstatite-magnesite-olivine-diamond) buffer retained up to 9 rel.% of alkanes and oxygenated HCs (Fig. 3).

The compositions of the synthesized C–O–H–N fluids depend on the material of capsules: Pt or Au (Sokol et al., 2017a). Pt capsules cause a catalytic effect: fluids obtained in these capsules have CH_4/C_2H_6 ratios slightly lower than those from the Au capsules, as well as low to zero concentrations of aldehydes and ketones that are consumed due to catalytical reactions on the Pt surface; however, the set of alkane species is generally similar in the fluids from the two capsule types.

Species diversity studies of reduced fluid often use thermodynamic calculations, and their interpretation jointly with experimental evidence is a powerful tool for understanding the features and mechanisms of the generation of reduced fluids. However, the review of thermodynamic calculations data is beyond the scope of this paper.

NITROGEN SPECIES IN FLUIDS

The formation and stability of ammonia (NH_3) in the fluid phase were studied in pressure and temperature ranges of 0.5 to 7.8 GPa and 600 to 1400 °C, respectively. The fluids synthesized in an N–O–H system contained more NH_3 under 0.2–3.5 GPa and 600–1400 °C at f_{O_2} about the IW buffer, but more N_2 at higher oxygen fugacities (Li and Keppler, 2014). In the 5.5–7.8 GPa and 1100–1500 °C *P–T* ranges, the concentrations of NH_3 and N_2 in model N-rich C–O–H–N fluids varied as a function of temperature, pressure, and f_{O_2} (Sokol et al., 2017b). Ammonia predominated in fluids generated in 6.3 GPa runs by thermal destruction of melamine ($C_3H_6N_6$) or its mixture with docosane ($C_{22}H_{46}$) or stearic acid ($C_{18}H_{36}O_2$) at –2 lg f_{O_2} ΔIW, whereas N_2 became the main nitrogen species already at +0.7 lg f_{O_2} ΔIW. Thus, the predominant nitrogen species in the model N-rich C–O–H–N fluids changed from NH_3 to N_2 as f_{O_2} was slightly above IW at 6.3 GPa and 1400 °C. The pressure variations from 5.5 to 7.8 GPa did not influence much the $NH_3/(NH_3+N_2)$ ratio in the fluids.

In experiments with the Fe–C–O–H–N system at 6.3–7.8 GPa and 1200–1400 °C, NH_3 was the predominant nitrogen species: $N_2/(NH_3+N_2) \le 0.36$ (Fig. 4). The hydrogen fugacity in the experiments was buffered by Fe–FeO + H_2O or Mo–MoO_2 + H_2O equilibria while f_{O_2} was constrained by the oxidation reactions of γ-Fe, metal melt, or iron nitride about the IW buffer. However, N_2 was superior ($N_2/(NH_3+N_2) = 0.91–0.99$) in the case of f_{O_2} buffered by an Fe–C–N melt and unbuffered f_{H_2} (f_{H_2} was controlled by the material of the high-pressure cell at about the Ni–NiO + H_2O equilibrium). Thus, low oxygen fugacity (about IW) is a necessary but not sufficient condition for NH_3 stability. In the *P–T* ranges applied in the runs, NH_3 can form at f_{H_2} much above Ni–NiO + H_2O. Note that the previous models (Li and Keppler, 2014; Sokol et al., 2017b) did not consider the role of f_{H_2} as a control of NH_3 stability.

The stability of main nitrogen species in fluids was studied in the system "lherzolite–C–O–H–N" at the *P–T* ranges 5.5 to 7.8 GPa and 1150 to 1350 °C and at f_{O_2} from –2.5 lg f_{O_2} ΔIW to the EMOD buffer and f_{H_2} from IW + H_2O to MH + H_2O. Ammonia predominated in the quenched fluid synthesized in a system of Fe^0-saturated lherzolite with added melamine at f_{H_2} about the IW + H_2O or MMO + H_2O equilibria, with the ratio $N_2/(NH_3+N_2) = 0.01–0.4$ (Fig. 5), as well as in the fluid where nitrogen came from air, at the same f_{O_2}–f_{H_2} redox conditions: $N_2/(NH_3+N_2) = 0.01–0.17$.

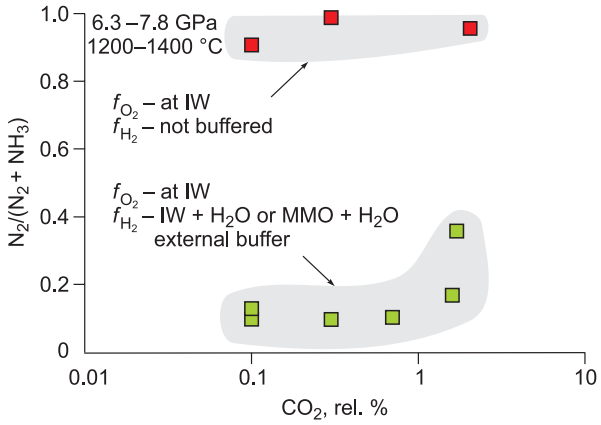

Fig. 4. N_2/NH_3 in quenched fluid synthesized in the system Fe–C–O–H–N as a function of CO_2 (at increasing f_{O_2}). Nitrogen comes from melamine which decomposed at the *P–T* conditions of the run as $C_3H_6N_6 \rightarrow 2NH_3 + 2N_2 + 3C$, after (Sokol et al., 2018b).

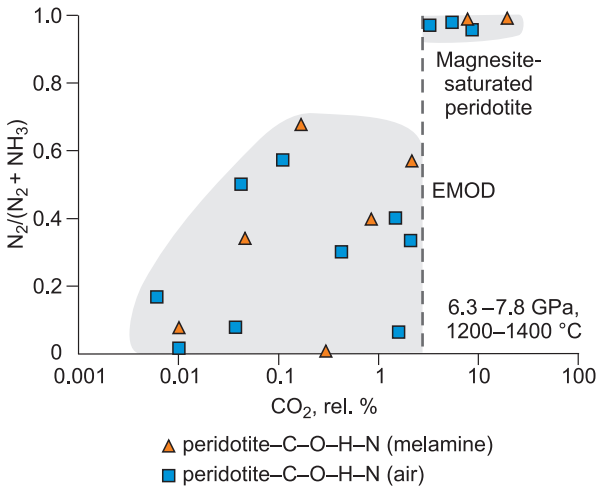

Fig. 5. N_2/NH_3 in quenched fluid synthesized in the system peridotite-C–O–H–N as a function of CO_2 (at increasing f_{O_2}). Nitrogen is from melamine and air N_2 (Sokol et al., 2018a). f_{H_2} was buffered by IW + H_2O and MMO + H_2O in runs with reduced peridotite and by MH+H_2O in runs with magnesite-bearing peridotite. EMOD is according to (Stachel and Luth, 2015).

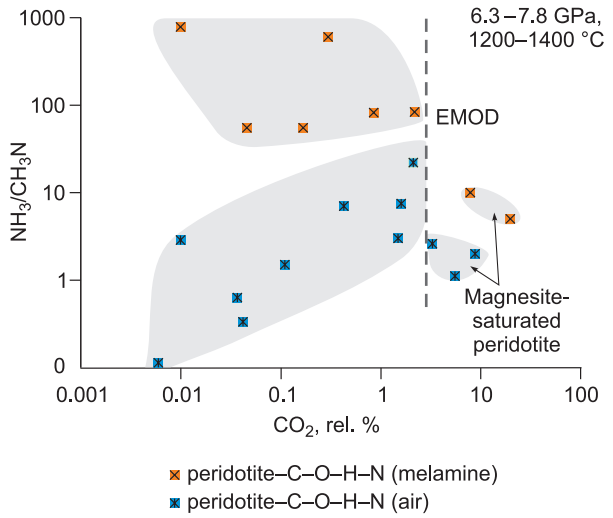

Fig. 6. NH_3/CH_3N in quenched fluid synthesized in the system peridotite-C–O–H–N as a function of CO_2 (at increasing f_{O_2}). Nitrogen is from melamine and air (Sokol et al., 2018a). f_{H_2} was buffered by IW + H_2O and MMO + H_2O in runs with reduced peridotite and by MH+H_2O in runs with magnesite-bearing peridotite. EMOD is according to (Stachel and Luth, 2015).

The $N_2/(NH_3 + N_2)$ ratio approached unity in 150 h runs, in oxidized conditions, in the presence of magnesite-saturated lherzolite at f_{H_2} buffered by MH + H_2O. The CO_2 contents in the analyzed fluids increased with f_{O_2}, and the contents of NH_3 decreased correspondingly (Fig. 5).

The N-bearing fluids synthesized at high pressures and temperatures (Sokol et al., 2017b, 2018a,b; 2019a,b) contained methanimine (CH_3N). Its presence in the quenched fluids obtained in a series of special experiments with the C–O–H–N system at 6.3 GPa and 1200 °C, in Au capsules, was detected by high-resolution mass spectrometry on a Thermo Fisher Scientific Double Focusing System (DFS) at the Institute of Organic Chemistry, Novosibirsk (Sokol et al., 2019b). It was marked by ions with m/z = 29.0250, with the assumed mass for the CH_3N $[M]^+$ molecular ion 29.0260, the mass for atmospheric nitrogen $[^{15}N^{14}N]^+$ being m/z = 29.0025. The concentration of CH_3N in the fluid was found out to depend mainly on redox conditions and the content of nitrogen in the system. Fluids enriched with nitrogen contained small amounts of CH_3N ($N_2/(CH_3N + N_2) > 0.9$), in both the Fe–C–O–H–N system (Sokol et al., 2018b) and in the Fe^0-bearing lherzolite samples (Fig. 6) (Sokol et al., 2018a). Moreover, NH_3 predominated over CH_3N in the whole applied range of f_{O_2}. Nevertheless, the amounts of CH_3N and NH_3 were often commensurate in N-poor fluids.

Thus, the experimental results evidence that significant NH_3 concentrations may occur in a fluid that is stable either in low-f_{O_2} subcratonic lithosphere or in Fe^0-bearing mantle. NH_3 is also controlled by hydrogen fugacity which should be at least at the MMO+H_2O equilibrium (Fig. 7): NH_3 cannot form in strongly reduced conditions at low f_{H_2}. Some nitrogen in N-poor reduced mantle fluids may reside in

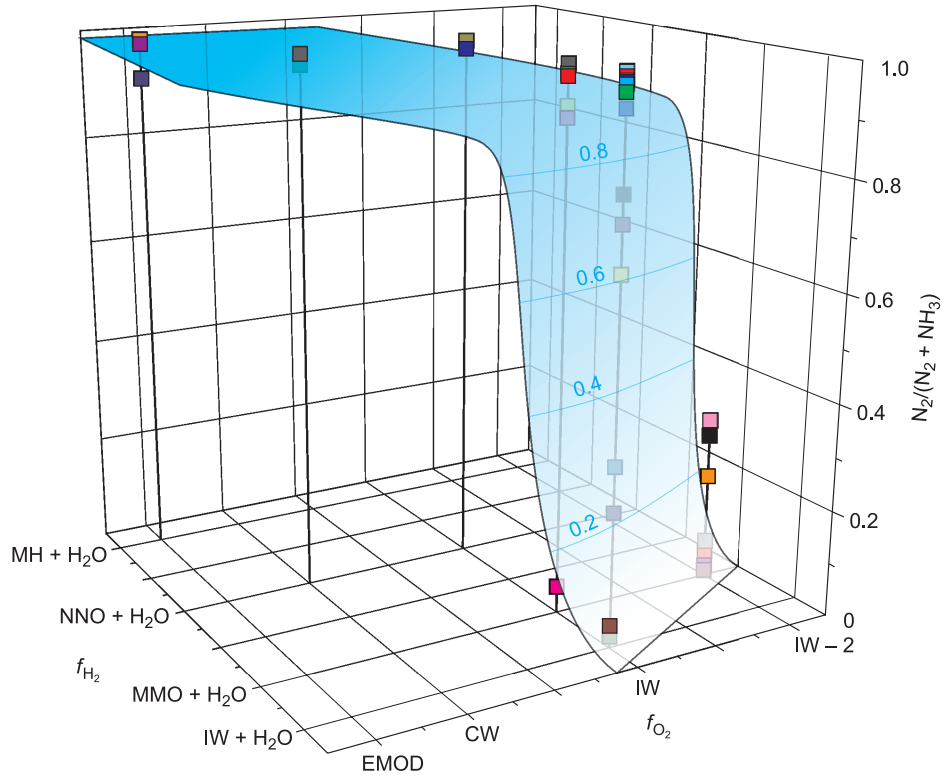

Fig. 7. Summary of experimental data on stability of NH_3 and N_2 in quenched fluids synthesized in systems C-O-H-N, Fe-C–O–H–N and peridotite-C–O–H–N (Sokol et al., 2017b, 2018a,b) at 5.5–7.8 GPa and 1150–1350 °C; oxygen fugacity is from –2.5 lg f_{O_2} ΔIW to EMOD and hydrogen fugacity is at IW+H_2O to MH + H_2O equilibria.

methanimine (CH_3N), which may approach the amounts of ammonia in fluids equilibrated with lherzolite. CH_3N may affect the mantle cycle of nitrogen because it does not participate in $(NH_4)^+ \rightarrow K^+$ substitutions and thus limits the solubility of nitrogen in silicates at low f_{O_2}. The stability limits of $(NH_4)^+$ and NH_3 in aqueous fluids from peridotite may also depend on pH (Mikhail and Sverjensky, 2014; Mikhail et al., 2017), but this issue is beyond the scope of the present study.

FLUID INCLUSIONS IN NATURAL DIAMOND

Fluid inclusions in deep-seated minerals analyzed by Raman or Fourier-transform infrared (FTIR) spectroscopy, scanning electron microscopy, microthermometry, and gas chromatography-mass spectrometry can provide evidence on the behavior of fluids in the mantle magmatic and metasomatic processes and diamond formation conditions (Sobolev and Lenskaya, 1965; Sobolev, 1989; Tomilenko et al., 2001, 2009, 2016a,b, 2018a; Cartigny, 2005; Klein-Ben David et al., 2007; Logvinova et al., 2011; Cartigny et al., 2014; Smith et al., 2014, 2015; Kaminsky et al., 2015; Sobolev et al., 2015, 2018, 2019a,b; Rudloff-Grund et al., 2016; Smith et al., 2016; Navon et al., 2017). Diamond is an exceptionally hard and chemically inert natural container which can maintain high pressure at room temperature inside fluid inclusions that were entrapped during crystallization (Roedder, 1984; Izraeli et al., 1999; Sobolev et al., 2000, 2015, 2019b; Navon et al., 2017). Raman and FTIR spectroscopy and microthermometry revealed methane, hydrogen, carbon dioxide, and nitrogen in fluid and melt inclusions from some diamonds (Tomilenko et al., 2001; Smith et al., 2014, 2015; Kaminsky et al., 2015; Sobolev et al., 2015, 2019b; Rudloff-Grund et al., 2016; Smith et al., 2016; Navon et al., 2017). Progress in using GC–MS for the past five years has extended our knowledge of volatiles in the Earth's upper mantle to 300 components. The fluid inclusions in kimberlite-hosted diamonds from Yakutia and in placer diamonds from the northeastern Siberian craton and the Ural Mountains contain hydrocarbons (alkanes, alkenes, naphthenes, and arenes) and their derivatives (alcohols or esters, aldehydes, ketones, and carboxylic acids) as main volatile components (Sobolev et al., 2015, 2018, 2019a,b; Tomilenko et al., 2018a). HCs in inclusions from both kimberlitic and placer diamonds may reach 79 rel.% and their derivatives may vary from 52 to 93 rel.% (Fig. 8). The contents of aliphatic hydrocarbons are from 18 rel.% in kimberlitic diamonds to 65 rel.% in placer diamonds from the two regions. Note that the concentrations of methane and other light alkanes (C_2–C_4) are minor (0.1–0.7 rel.%) in all cases. Oxygenated hydrocarbons are quite high, from 56 rel.% in kimberlitic to 65 rel.% in placer diamonds.

The contents of water are quite low and CO_2 varies depending on the origin of diamonds: those from the Yakutain kimberlites contain ~ 12 rel.% H_2O and 0.3 to 7 rel.% CO_2, whereas the respective values for diamonds from the northeastern Siberia and Ural placers are 0.4 to 10 rel.% H_2O and 2 to 29 rel.% CO_2 (Sobolev et al., 2018, 2019a,b; Tomilenko et al., 2018a). The compositions of volatiles are compared in Fig. 8 for peridotitic diamond from the Udachnaya kimberlite (Sobolev et al., 2019a) and eclgitic diamond from plac-

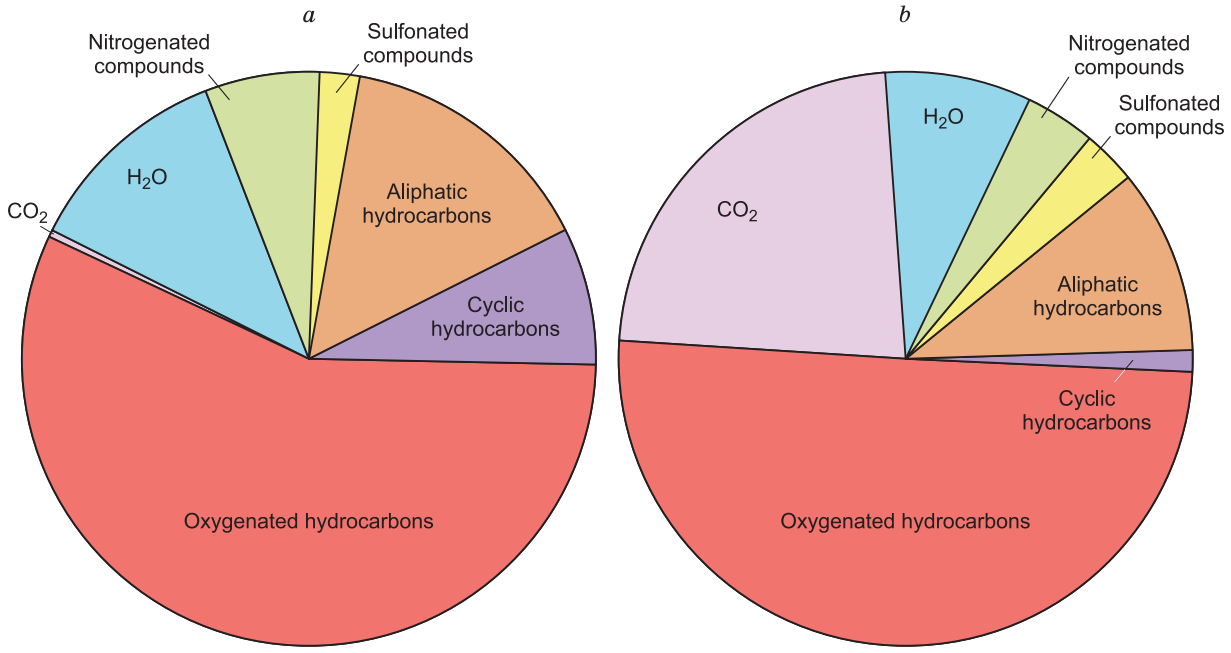

Fig. 8. Relative percentages of volatiles in fluid inclusions from natural diamonds, according to GC-MS. *a*, Peridotitic diamond, xenolith in Udachnaya kimberlite (Sobolev et al., 2019a); *b*, eclgitic diamond, placers in northeastern Siberian craton (Tomilenko et al., 2018a).

ers in the northeastern Siberian craton (Tomilenko et al., 2018a). The H/(O + H) ratios in the Yakutian kimberlitic diamonds and in the placer diamonds (both regions) range from 0.74 to 0.93 (Sobolev et al., 2018, 2019a,b; Tomilenko et al., 2018a). The estimated range of f_{O_2} variations in the mantle growth medium of diamond is from strongly reduced (below IW) to about the EMOD buffer, judging by CO_2 in fluid inclusions. The discovered variations in the H_2O and CO_2 contents and HC diversity may be due to redox reactions in the mantle.

The behavior of nitrogen in mantle fluids has implications for its possible participation in diamond formation. GC–MS revealed molecular nitrogen in all diamonds from the Yakutian kimberlite and from placers in the northeastern Siberia and Ural regions, as well as 24 nitrogen species, including amines, amides, imides, nitriles, and other homologs (Tomilenko et al., 2001, 2018a; Sobolev et al., 2015, 2018, 2019a,b). Therefore, nitrogen was present in the natural mineral-forming medium as N_2 or NH_x-ions, and molecular nitrogen was commonly inferior to the ionic form in both kimberlitic and placer diamonds, except for sublithospheric placer diamonds from the Ural. Note that none of the natural diamond sample contained ammonia or methanimine (Tomilenko et al., 2018a; Sobolev et al., 2018, 2019a,b).

Diamond from mantle xenoliths in kimberlites often encloses sulfides (Meyer, 1987; Bulanova et al., 1996). The occurrence of metal-carbon-sulfide melt inclusions in natural diamond provides direct evidence that sulfur compounds were involved in diamond formation at mantle depths (Smith et al., 2016). Sulfur has been recognized to be a common component in C–O–H–N–S deep fluids (Thomassot et al., 2007, 2009; Taylor and Liu, 2009; Tsuno and Dasgupta, 2015), but the presence of volatile sulfur compounds in the mantle was proved only by recent GC–MS analyses of fluid inclusions from diamond. Namely, 3 to 16 sulfur species, 0.2 to 9 rel.%, were found in kimberlite-hosted diamond from Yakutia and in placer diamond from northeastern Siberia and the Urals: SO_2, COS, CS_2, $C_2H_6S_2$, and diverse thiophenes from 2-methylthiophene (C_5H_6S) to 3-butylthiophene ($C_8H_{12}S$), etc. (Tomilenko et al., 2018a; Sobolev et al., 2018, 2019a,b).

Almost all fluid inclusions in natural diamonds also contain Cl-bearing hydrocarbons: mostly Cl-bearing alkanes, as well as less abundant alkenes, cyclic hydrocarbons, and esters, occasionally up to 3.5 rel.% in total (Tomilenko et al., 2018a; Sobolev et al., 2018, 2019a,b). Their discovery has demonstrated that Cl-bearing HCs are stable in the upper mantle and that reduced fluids can be efficient chlorine carriers, which has important implications for the deep chlorine cycle.

It is interesting to compare the species composition of volatiles in inclusions from natural diamond with those from synthetic diamond grown at high pressures and temperatures (HPHT) in metal-carbon systems (Palyanov et al., 2010; Tomilenko et al., 2018b,c) or synthesized by chemical vapor deposition (CVD) (Tomilenko et al., 2019). The primary fluid inclusions and volatile melt inclusions in synthetic monocrystals of HPHT and CVD diamonds consist mainly of hydrocarbons and their derivatives, up to 87 rel.% in total. The synthetic diamonds of both types contain aliphatic (alkanes and alkenes), cyclic (naphthenes and arenes), and oxygenated (alcohols, esters, aldehydes, ketones, and carboxylic acids) HCs, as well as compounds bearing N, Cl, and S. Note that the concentrations of oxygenated hydrocarbons are high in both natural and synthetic diamonds: up to 64 rel.%. The calculated H/(O + H) ratios for fluid inclusions in synthetic diamonds are from 0.82 to 0.93 (Tomilenko et al., 2018b,c, 2019) and overlap with those for some natural kimberlitic and placer diamonds. This overlap indicates that the metal–carbon systems generating synthetic diamond and the growth media of natural mantle diamond share redox similarity.

CONCLUSIONS

The available experimental results show that hydrocarbons, mainly light alkanes, are stable at mantle pressures and temperatures, in both simplified fluid and more complex peridotite-fluid systems, at redox conditions from ultra-reduced to +2 lg $f_{O_2}\Delta$IW (water maximum level). Carboxylic acids and other O-bearing HCs can be stable even in $H_2O + N_2 + CO_2$ fluids equilibrated with carbonate-bearing peridotite. Hydrocarbons can form either by reactions of carbonates with water and metallic iron or wüstite, or by direct hydrogenation of carbon phases (graphite, diamond, amorphous carbon) upon their interaction with fluids, at buffered f_{H_2}. Carbon may come from various mantle minerals: carbonates, diamond, or graphite. The experimental data prove the possibility of abiotic HC generation in the volatile-rich reduced mantle of terrestrial planets, including in the early Earth. Favorable conditions for HC generation may exist in zones where slab-derived fluids interact with Fe^0-bearing mantle. The deep-seated fluids may contain ammonia (NH_3) either in relatively reduced subcratonic lithosphere or in Fe^0-bearing mantle at high fH_2, and methanimine (CH_3N) in N-poor varieties of reduced fluids.

The presence of hydrocarbons as key constituents of reduced mantle fluids has been proven by data on inclusions in natural kimberlitic diamond from the Yakutian province and placer diamond from the northeastern Siberian craton and the Urals. The fluids entrapped in natural diamonds have H/(H+O) ratios from 0.74 to 0.93 and contain low amounts of methane and other light alkanes at high contents of oxygenated HCs; <12 rel.% H_2O and up to 29 rel.% CO_2 (in eclogitic diamonds); molecular nitrogen and N-bearing compounds (amines, primary amides, imides, nitriles, etc.), but no ammonia; Cl- and sulfur-bearing compounds.

Integration of data on experimental model systems and inclusions from natural diamonds makes an important step toward understanding the mantle fluid regime. The key inference is that hydrocarbons were stable in reduced fluids in

the upper mantle, specifically, in the growth medium of some mantle diamonds. Diverse HCs in the mantle, mainly light alkanes and oxygenated HC species, can have formed from inorganic substances, with participation of N-, S-, and Cl-bearing compounds.

Future research may focus on the trends of fluid composition changes in inclusions from diamonds carried to the surface; the causes of difference between experimental and natural systems in relative percentages of HC species and water; and stability of N-, S, and Cl-bearing fluid components.

This research was partly supported by grants 16-17-10041 and 19-17-00128 from the Russian Science Foundation and by grant 18-05-00761 from the Russian Foundation for Basic Research.

REFERENCES

Bebout, G.E., Lazzeri, K.E., Geiger, C.A., 2016. Pathways for nitrogen cycling in Earth's crust and upper mantle: a review and new results for microporous beryl and cordierite. Am. Mineral. 101, 7–24.

Benedetti, L.R., Nguyen, J.H., Caldwell, W.A., Liu, H., Kruger, M., Jeanloz, R., 1999. Dissociation of CH_4 at high pressures and temperatures: diamond formation in giant planet interiors? Science 286 (5437), 100–102.

Bulanova, G.P., Griffin, W.L., Ryan, C.G., Shestakova, O.Y. Barnes S.J., 1996. Trace elements in sulfide inclusions from Yakutian diamonds. Contrib. Mineral. Petrol. 124 (2), 111–125.

Busigny, V., Cartigny, P., Philippot, P., Ader, M., Javoy, M., 2003. Massive recycling of nitrogen and other fluid-mobile elements (K, Rb, Cs, H) in a cold slab environment: evidence from HP to UHP oceanic metasediments of the Schistes Lustres nappe (western Alps, Europe). Earth Planet. Sci. Lett. 215 (1–2), 27–42

Canil, D., O'Neill, H.St.C., 1996. Distribution of ferric iron in some upper-mantle assemblages. J. Petrol. 37, 609–635.

Cartigny, P., 2005. Stable isotopes and the origin of diamond. Elements 1, 79–84.

Cartigny, P., Palot, M., Thomassot, E., Harris, J.W., 2014. Diamond formation: a stable isotope perspective. Ann. Rev. Earth Planet. Sci. 42 (1), 699–732.

Creighton, S., Stachel, T., Matveev, S., Höfer, H., McCammon, C., Luth, R.W., 2009. Oxidation of the Kaapvaal lithospheric mantle driven by metasomatism. Contrib. Mineral. Petrol. 157 (4), 491–504.

Creighton, S., Stachel, T., Eichenberg, D., Luth, R.W., 2010. Oxidation state of the lithospheric mantle beneath Diavik diamond mine, central Slave craton, NWT, Canada. Contrib. Mineral. Petrol. 159 (5), 645–657.

Elkins, L.J., Fischer, T.P., Hilton, D.R., Sharp, Z.D., McKnight, S., Walker, J., 2006. Tracing nitrogen in volcanic and geothermal volatiles from the Nicaraguan volcanic front. Geochem. Cosmochim. Acta 70 (20), 5215–5235.

Etiope, G., Sherwood Lollar, B., 2013. Abiotic methane on Earth. Rev. Geophys. 51 (2), 276–299.

Fedorov, I.I., Chepurov, A.I., Osorgin, N.Yu., Sokol, A.G., Sobolev N.V., 1991. Experimental and thermodynamic modeling of the C-O-H fluids in equilibrium with graphite and diamond at high P–T parameters. Dokl. Akad. Nauk SSSR 320, 710–712.

Frost, D.J., Liebske, C., Langenhorst, F., McCammon, C.A., Tronnes, R.G., Rubie, D.C., 2004. Experimental evidence for the existence of iron-rich metal in the Earth's lower mantle. Nature 248, 409–412.

Frost, D.J., McCammon, C.A., 2008. The redox state of Earth's mantle. Ann. Rev. Earth Planet. Sci. 36, 389–420.

Goncharov, A.G., Ionov, D.A., Doucet, L.S., Pokhilenko, L.N., 2012. Thermal state, oxygen fugacity and C–O–H fluid speciation in cratonic lithospheric mantle: new data on peridotite xenoliths from the Udachnaya kimberlite, Siberia. Earth Planet. Sci. Lett. 357, 99–110.

Halama, R., Bebout, G.E., John, T., Schenk, V., 2010. Nitrogen recycling in subducted oceanic lithosphere: the record in high-and ultra-high-pressure metabasaltic rocks. Geochem. Cosmochim. Acta 74 (5), 1636–1652.

Izraeli, E.S., Harris, J.W., Navon, O., 1999. Raman barometry of diamond inclusions. Earth Planet. Sci. Lett. 173, 351–360.

Kadik, A.A., 2003. Reduced fluids in the mantle: relation with chemical differentiation of the planetary material. Geochem. Int. 41, 844–855.

Kaminsky, F.V., Wirth, R., Schreiber, A., 2015. A microinclusion of lower-mantle rock and other minerals and nitrogen lower-mantle inclusions in a diamond. Can. Mineral. 53, 83–104.

Kenney, J.F., Kutcherov, V.A., Bendeliani, N.A, Alekseev, V.A., 2002. The evolution of multicomponent systems at high pressures: the thermodynamic stability of the hydrogen-carbon system: the genesis of hydrocarbons and the origin of petroleum. Proc. Nat. Acad. Sci. U.S.A. 99, 10976–10981.

Klein-Ben David, O., Izraeli, E.S., Hauri, E., Navon, O., 2007. Fluid inclusions in diamonds from the Diavik mine, Canada, and the evolution of diamond-forming fluids. Geochim. Cosmochim. Acta 71, 723–744.

Kolesnikov, A., Kutcherov, V.G., Goncharov, A.F., 2009. Methane-derived hydrocarbons produced under upper-mantle conditions. Nat. Geosci. 2 (8), 566–570.

Kolesnikov, A.Y., Saul, J.M., Kutcherov, V.G., 2017. Chemistry of hydrocarbons under extreme thermobaric conditions. Chemistry Select 2, 1336–1352.

Kucherov, V.G., Kolesnikov, A.Yu., Dyuzheva, T.I., Kulikova, L.F., Nikolaev, N.N., Sazanova, O.A., Brazhkin, V.V., 2010. Synthesis of complex hydrocarbon systems at temperatures and pressures corresponding to the Earth's upper mantle conditions. Dokl. Phys. Chem. 433 (1), 132–135.

Lazarov, M., Woodland, A.B., Brey, G.P., 2009. Thermal state and redox conditions of the Kaapvaal mantle: a study of xenoliths from the Finsch mine, South Africa. Lithos 112S, 913–923.

Li, Y., Keppler, H., 2014. Nitrogen speciation in mantle and crustal fluids. Geochem. Cosmochim. Acta 129, 13–32.

Li, Y., Wiedenbeck, M., Shcheka, S., Keppler, H., 2013. Nitrogen solubility in upper mantle minerals. Earth Planet Sci. Lett. 377, 311–323.

Li, Y, Huang, R, Wiedenbeck, M, Keppler, H., 2015. Nitrogen distribution between aqueous fluids and silicate melts. Earth Planet Sci. Lett. 411, 218–228.

Litasov, K.D., Shatskiy, A.F., Ohtani, E., 2014. Melting and subsolidus phase relations in peridotite and eclogite systems with reduced C–O–H fluid at 3–16 GPa. Earth Planet Sci. Lett. 391, 87–99.

Lobanov, S.S., Chen, P.N., Chen, X.J., Zha, C.S., Litasov, K.D., Mao, H.K., Goncharov, A.F., 2013. Carbon precipitation from heavy hydrocarbon fluid in deep planetary interiors. Nat. Commun. 4, 2466–2473.

Logvinova, A.M., Virt, R., Tomilenko, A.A., Afanasiev, V.P., Sobolev, N.V., 2011. The phase composition of crystal-fluid nanoinclusions in alluvial diamonds in the northeastern Siberian Platform. Russian Geology and Geophysics (Geologiya i Geofizika) 52 (11), 1286–1298 (1634–1648).

Luth, R.W., 2014. Volatiles in Earth's mantle, in: Treatise on Geochemistry. Elsevier, Oxford, pp. 355–391.

Luth, R.W., Virgo, D., Boyd, F.R., Wood, B.J., 1990. Ferric iron inmantle-derived garnets. Contrib. Mineral. Petrol. 104 (1), 56–72.

Mallik, A., Li, Y., Wiedenbeck, M., 2018. Nitrogen evolution within the Earth's atmosphere: mantle system assessed by recycling in subduction zones. Earth Planet. Sci. Lett. 482, 556–566.

Matjuschkin, V., Woodland, A.B., Yaxley, G.M., 2019. Methane-bearing fluids in the upper mantle: an experimental approach. Contrib. Mineral. Petrol. 174 (1), 1–14.

Matveev, S., Ballhaus, C., Fricke, K., Truckenbrodt, J., Ziegenben, D., 1997. Volatiles in the Earth's mantle: I. Synthesis of CHO fluids at 1273 K and 2.4 GPa. Geochim. Cosmochim. Acta 61, 3081–3088.

McCammon, C.A., Kopylova, M.G., 2004. A redox profile of the Slave mantle and oxygen fugacity control in the cratonic mantle. Contrib. Mineral. Petrol. 148 (1), 55–68.

Meyer, H.O.A., 1987. Inclusions in Diamonds, in: Nixon, P.H. (Ed.), Mantle Xenoliths, John Willey & Sons, Chichester, pp. 501–522.

Mikhail, S., Sverjensky, D.A., 2014. Nitrogen speciation in upper mantle fluids and the origin of Earth's nitrogen-rich atmosphere. Nat. Geosci. 7, 816–819.

Mikhail, S., Barry, P.H., Sverjensky, D.A., 2017. The relationship between mantle pH and the deep nitrogen cycle. Geochim. Cosmochim. Acta 209, 149–160.

Mukhina, E., Kolesnikov, A., Kutcherov, V., 2017. The lower pT limit of deep hydrocarbon synthesis by CaCO3 aqueous reduction. Sci. Rep. 7, 5749–5754.

Mysen, B., 2019. Nitrogen in the Earth: abundance and transport. Progress Earth Planet. Sci. 6 (1), 38–53.

Navon, O., Wirth, R., Schmidt, C., Jablon, B. M., Schreiber, A., Emmanuel, S., 2017. Solid molecular nitrogen (d-N2) inclusions in Juina diamonds: Exsolution at the base of transition zone. Earth Planet. Sci. Lett. 464, 237–247.

Palyanov, Y.N., Borzdov, Y.M., Kupriyanov, I.N., Khokhryakov, A.F., 2010. Effect of H_2O on diamond crystal growth in metal–carbon systems. Cryst. Growth Des. 12 (11), 5571–5578.

Roedder, E., 1984. Fluid inclusions. Reviews in mineralogy. Mineralogical Society of America. Vol. 12.

Rohrbach, A., Ballhaus, C., Golla–Schindler, U., Ulmer, P., Kamenetsky, V. S., Kuzmin, D.V., 2007. Metal saturation in the upper mantle. Nature 449, 456–458.

Rohrbach, A., Schmidt, M.W., 2011. Redox freezing and melting in the Earth's deep mantle resulting from carbon-iron redox coupling. Nature 472, 209–212.

Rudloff-Grund, J., Brenker, F.E., Marquardt, K., Howell, D., Schreiber, A., O'Reilly, S.Y., Griffin, W.L., Kaminsky, F.V., 2016. Nitrogen nanoinclusions in milky diamonds from Juina area, Mato Grosso State, Brazil. Lithos 265, 57–67.

Scott, H.P., Hemley, R.J., Mao, H., Herschbach, D.R., Fried, L.E., Howard, W.M., Bastea, S., 2004. Generation of methane in the Earth's mantle: *In situ* high pressure–temperature measurements of carbonate reduction. Proc. Nat. Acad. Sci. U.S.A. 101, 14023–14026.

Sharma, A., Cody, G.D., Hemley, R.J., 2009. *In situ* diamond-anvil cell observations of methanogenesis at high pressures and temperatures. Energy and Fuels 23 (11), 5571–5579.

Shirey, S.B., Cartigny, P., Frost, D. J., Keshav, S., Nestola, F., Nimis, P., Pearson, D.G., Sobolev, N.V., Walter, M. J., 2013. Diamonds and the geology of mantle carbon. Rev. Mineral. Geochem. 75 (1), 355–421.

Smith, E.M., Kopylova, M.G., Frezzotti, M.L., Afanasiev, V.P., 2014. N-rich fluid inclusions in octahedrally-grown diamond. Earth Planet. Sci. Lett. 393, 39–48.

Smith, E.M., Kopylova, M.G., Frezzotti, M.L., Afanasiev, V.P., 2015. Fluid inclusions in Ebelyakh diamonds: Evidence of CO_2 liberation in eclogite and the effect of H_2O on diamond habit. Lithos 216–217, 106–117.

Smith, E.M., Shirey, S.B., Nestola, F., Bullock, E.S., Wang, J., Richardson, S.H., Wang W., 2016. Large gem diamonds from metallic liquid in Earth's deep mantle. Science 354 (6318), 1403–1405.

Sobolev, E.V., 1989. Harder than the Diamond [in Russian]. Nauka, Novosibirsk, 192.

Sobolev, E.V., Lenskaya, S.V., 1965. On the manifestation of "gas" impurities in the spectra of natural diamonds. Geologiya i Geofizika 2, 157–159.

Sobolev, N.V., Fursenko, B.A., Goryainov, S.V., Shu, J., Hemley, R.J., Mao, A., Boyd, F.R., 2000. Fossilized high pressure from the Earth's deep interior: the coesite-in-diamond barometer. Proc. Natl. Acad. Sci U.S.A. 97 (22), 11875–118879.

Sobolev, N.V., Logvinova, A.M., Fedorova, E.N., Lukyanova, L.I., Wirth, R., Tomilenko, A.A., Bulbak, T.A., Reutsky, V.N., Efimova, E.S., 2015. Mineral and fluid inclusions in the diamonds from the Ural placers, Russia, in: AGU Fall Meeting, Abstr. V11C–3073.

Sobolev, N.V., Sobolev, A.V., Tomilenko, A.A, Kuz'min, D.V., Grakhanov, S.A, Batanova, V.G., Logvinova, A.M., Bul'bak, T.A., Kostrovitskii, S.I., Yakovlev, D.A., Fedorova, E.N., Anastasenko, G.F., Nikolenko, E.I., Tolstov, A.V., Reutskii, V.N., 2018. Prospects of search for diamondiferous kimberlites in the northeastern Siberian Platform. Russian Geology and Geophysics (Geologiya i Geofizika) 59 (10), 1365–1379 (1701–1719).

Sobolev, N.V., Logvinova, A.M., Tomilenko, A.A., Wirth, R., Bulbak, T.A., Lukyanova, L.I., Fedorova, E.N., Reutsky, V.N., Efimova, E.S., 2019a. Mineral and fluid inclusions in diamonds from the Urals placers, Russia: Evidence for solid molecular N_2 and hydrocarbons in fluid inclusions. Geochim. Cosmochim. Acta 266, 197–219.

Sobolev, N.V., Tomilenko, A.A., Bulbak, T.A., Logvinova, A.M., 2019b. Composition of hydrocarbons in diamonds, garnet, and olivine from diamondiferous peridotites from the Udachnaya pipe in Yakutia, Russia. Engineering 5, 471–478

Sobolev, V.S., 1960. The conditions of diamond formation. Geologiya i Geofizika 1, 7–22.

Sokol, A.G., Palyanov, Y.N., Palyanova, G.A., Tomilenko, A.A., 2004. Diamond crystallization in fluid and carbonate-fluid systems under mantle PT conditions: 1. Fluid composition. Geochem. Int. 42 (9), 830–838.

Sokol, A.G., Palyanova, G.A., Palyanov, Y.N., Tomilenko, A.A., Melenevsky, V.N., 2009. Fluid regime and diamond formation in the reduced mantle: experimental constraints. Geochim. Cosmochim. Acta 73, 5820–5834.

Sokol, A.G., Tomilenko, A.A., Bulbak, T.A., Palyanova, G.A., Sokol, I.A., Palyanov, Y.N., 2017a. Carbon and nitrogen speciation in N-poor C–O–H–N fluids at 6.3 GPa and 1100–1400 °C. Sci. Rep. 7, 1–19.

Sokol, A.G., Palyanov, Y.N., Tomilenko, A.A., Bulbak, T.A., Palyanova, G.A., 2017b. Carbon and nitrogen speciation in nitrogen-rich C–O–H–N fluids at 5.5–7.8 GPa. Earth Planet. Sci. Lett. 460, 234–243.

Sokol, A.G., Tomilenko, A.A., Bulbak, T.A., Kruk, A.N., Sokol, I.A., Palyanov, Y.N., 2018a. Fate of fluids at the base of subcratonic lithosphere: Experimental constraints at 5.5–7.8 GPa and 1150–1350 deg C. Lithos 318, 419–433.

Sokol, A.G., Tomilenko, A.A., Bulbak, T.A., Kruk, A.N., Zaikin, P.A., Sokol, I.A., Seryotkin, Y.V., Palyanov, Y.N., 2018b. The Fe–C–O–H–N system at 6.3–7.8 GPa and 1200–1400 °C: implications for deep carbon and nitrogen cycles. Contrib. Mineral. Petrol. 173 (6), Article 47.

Sokol, A.G., Kupriyanov, I.N., Tomilenko, A.A., Bulbak, T.A., Palyanov, Yu.N., Sobolev, N.V., 2018c. Formation of water-bearing defects in olivine in the presence of water-hydrocarbon fluid at 6.3 GPa and 1200 °C. Dokl. Earth Sci. 483 (1), 1451–1453.

Sokol, A.G., Tomilenko, A.A., Bulbak, T.A., Sokol, I.A., Zaikin, P.A., Palyanova, G.A., Palyanov, Y.N., 2019a. Hydrogenation of carbon at 5.5–7.8 GPa and 1100–1400 °C: Implications to formation of hydrocarbons in reduced mantles of terrestrial planets. Phys. Earth Planet. Inter. 291, 12–23.

Sokol, I., Sokol, A., Bulbak, T., Nefyodov, A., Zaikin, P., Tomilenko, A., 2019b. C-and N-bearing species in reduced fluids in the simplified C–O–H–N system and in natural pelite at upper mantle P–T conditions. Minerals 9 (11), 712–729.

Sonin, V.M., Bulbak, T.A., Zhimulev, E.I., Tomilenko, A.A., Chepurov, A.I., Pokhilenko, N.P., 2014. Synthesis of heavy hydrocarbons under P–T conditions of the Earth's upper mantle. Dokl. Earth Sci. 454 (1), 32–36.

Spanu, L., Donadio, D., Hohl, D., Schwegler, E., Galli, G., 2011. Stability of hydrocarbons at deep Earth pressures and temperatures. Proc. Nat. Acad. Sci. U.S.A. 108, 6843–6846.

Stachel, T., Luth, R.W., 2015. Diamond formation – where, when and how? Lithos 220, 200–220.

Stagno, V., Ojwang, D.O., McCammon, C.A., Frost, D.J., 2013. The oxidation state of the mantle and the extraction of carbon from Earth's interior. Nature 493, 84–88.

Sverjensky, D.A., Stagno, V., Huang, F., 2014. Important role for organic carbon in subduction-zone fluids in the deep carbon cycle. Nat. Geosci. 7, 909–914.

Tao, R., Zhang, L., Tian, M., Zhu, J., Liu, X., Liu, J., Höfer, H.E., Stagno, V., Fei, Y., 2018. Formation of abiotic hydrocarbon from reduction of carbonate in subduction zones: Constraints from petrolgical observation and experimental simulation. Geochim. Cosmochim. Acta 239, 390–408.

Taylor, L.A., Liu, Y., 2009. Sulfide inclusions in diamonds: not monosulfide solid solution. Russian Geol. Geophys. 50, 1201–1211.

Thomassot, E., Cartigny, P., Harris, J.W., Viljoen, K.S., 2007. Methane related diamond crystallization in the Earth's mantle: Stable isotope evidences from a single diamond-bearing xenolith. Earth Planet. Sci. Lett. 257, 362–371.

Thomassot, E., Cartigny, P., Harris, J.W., Lorand, J.P., Rollion-Bard, C., Chaussidon, M., 2009. Metasomatic diamond growth: A multi-isotope study (^{13}C, ^{15}N, ^{33}S, ^{34}S) of sulphide inclusions and their host diamonds from Jwaneng (Botswana). Earth Planet. Sci. Lett. 282, 79–90.

Tomilenko, A.A., Ragozin, A.L., Shatskiy, V.S., Shebanin, A.P., 2001. Variations in the fluid phase composition in the process of natural diamond crystallization. Dokl. Earth Sci. 379, 571–574.

Tomilenko, A.A., Kovyazin, S.V., Pokhilenko, L.N., Sobolev, N.V., 2009. Primary hydrocarbon inclusions in garnet of diamondiferous eclgite from the Udachnaya kimberlite pipe, Yakutia. Dokl. Earth Sci. 426 (1), 695–698.

Tomilenko, A.A., Bulbak, T.A., Khomenko, M.O., Kuzmin, D.V., Sobolev, N.V., 2016a. The composition of volatile components in olivines from Yakutian kimberlites of various ages: evidence from gas chromatography-mass spectrometry. Dokl. Earth Sci. 468 (2), 626–631.

Tomilenko, A.A., Bulbak, T.A., Polhilenko, L.N., Kuzmin, D.V., Sobolev, N.V., 2016 b. Peculiarities of the composition of volatile components in picroilmenites from Yakutian kimberlites of various ages (by gas chromatography-mass spectrometry). Dokl. Earth Sci. 469 (1), 690–694.

Tomilenko, A.A., Bulbak, T.A., Logvinova A.M., Sonin V.M., Sobolev N.V., 2018a. The composition features of volatile components in diamonds from the placers in the northeastern part of the Siberian Platform by gas chromatography-mass spectrometry. Dokl. Earth Sci. 481 (1), 953–957.

Tomilenko, A.A., Bulbak, T.A., Chepurov, A.I., Sonin, V.M., Zhimulev, E.I., Pokhilenko, N.P., 2018b. Composition of hydrocarbons in synthetic diamonds grown in a Fe-Ni-C system (according to gas chromatography-mass spectrometry data). Dokl. Earth Sci. 481 (2), 1004–1007.

Tomilenko, A.A. Zhimulev, E.I., Bulbak, T.A., Sonin, V.M., Chepurov, A.I., Pokhilenko, N.P., 2018c. Peculiarities of the composition of volatiles of diamonds synthesized in the Fe–S–C system: data on gas chromatography-mass spectrometry. Dokl. Earth Sci. 482 (1), 1207–1211.

Tomilenko, A., Sonin, V., Bulbak, T., Chepurov, A., 2019. Composition of volatile components in the polycrystalline CVD diamond (by coupled gas chromatographic–mass spectrometric analysis). Carbon Letters 29, 327–336.

Tsuno, K., Dasgupta, R., 2015. Fe–Ni–Cu–C–S phase relations at high pressures and temperatures – The role of sulfur in carbon storage and diamond stability at mid-to deep-upper mantle. Earth Planet. Sci. Lett. 412, 132–142.

Watenphul, A., Wunder, B., Heinrich, W., 2009. High-pressure ammonium-bearing silicates: implications for nitrogen and hydrogen storage in the Earth's mantle. Am. Mineral. 94, 283–292.

Watenphul, A., Wunder, B., Wirth, R., Heinrich, W., 2010. Ammonium-bearing clinopyroxene: a potential nitrogen reservoir in the Earth's mantle. Chem. Geol. 270, 240–248.

Woodland, A.B., Koch, M., 2003. Variation in oxygen fugacity with depth in the upper mantle beneath Kaapvaal craton, South Africa. Earth Planet. Sci. Lett. 214, 295–310.

Yaxley, G.M., Berry, A.J., Kamenetsky, V.S., Woodland, A. B. Golovin, A.V., 2012. An oxygen fugacity profile through the Siberian Craton-Fe K-edge XANES determinations of $Fe^{3+}/\Sigma Fe$ in garnets in peridotite xenoliths from the Udachnaya East kimberlite. Lithos 140–141, 142–151.

Zerkle, A.L., Mikhail, S., 2017. The geobiological nitrogen cycle: from microbes to the mantle. Geobiology 15 (3), 343–352.

Editorial responsibility: V.S. Shatsky